Annu. Rev. Biophys. Biomol. Struct. 2002. 31:275–302
DOI: 10.1146/annurev.biophys.31.101101.140927

PRINCIPLES AND BIOPHYSICAL APPLICATIONS OF LANTHANIDE-BASED PROBES

Paul R. Selvin
Physics Department and Biophysics Group, University of Illinois, Urbana, Illinois 61801; e-mail: selvin@uiuc.edu

Key Words fluorescence resonance energy transfer, lanthanide, luminescence

■ **Abstract** Using luminescent lanthanides, instead of conventional fluorophores, as donor molecules in resonance energy transfer measurements offers many technical advantages and opens up a wide range of new applications. Advantages include farther measurable distances (∼100 Å) with greater accuracy, insensitivity to incomplete labeling, and the ability to use generic relatively large labels, when necessary. Applications highlighted include the study of ion channels in living cells, protein-protein interaction in cells, DNA-protein complexes, and high-throughput screening assays to measure peptide dimerization associated with DNA transcription factors and ligand-receptor interactions.

CONTENTS

INTRODUCTION TO LANTHANIDE LUMINESCENCE AND ITS APPLICATIONS

Luminescent lanthanide chelates have highly unusual spectral characteristics that make them useful nonisotopic alternatives to organic fluorophores, particularly where there are problems of background autofluorescence (40, 53). They are also useful donors in fluorescence (luminescence) resonance energy transfer to measure nanometer conformational changes and binding events (42, 50, 57). In this review we focus on the use of lanthanides in energy transfer experiments.

Fluorescence resonance energy transfer (FRET) is a widely used technique to measure the distance between two points separated by approximately 15–100 Å (10, 12, 16, 49, 51). Measurements can be done under physiological conditions in vitro and especially with genetically encoded dyes, often in vivo as well. The technique relies on a distant-dependent transfer of energy from a donor fluorophore to an acceptor dye. Energy transfer leads to spectral changes, including changes in donor intensity, excited-state lifetime, and photobleaching rates, as well as acceptor changes. By monitoring these changes, the amount of energy transfer can be deduced, and with suitable calibrations one can then infer the distance. FRET has generally relied on organic-based dyes. However, a recent modification of the technique uses a luminescent lanthanide donor to transfer energy to an (organic-based) acceptor dye. Because lanthanide emission is technically not fluorescence (i.e., arising from a singlet-to-singlet transition), this has been called lanthanide-based or luminescence resonance energy transfer (LRET). LRET has a number of technical advantages compared to conventional FRET but relies on the same fundamental mechanism: subject to careful interpretation of various terms. Technical advantages include larger measurable distance range (>100 Å), with significantly greater accuracy and signal to background, and insensitivity to incomplete probe labeling.

First we briefly discuss the luminescent and photophysical characteristics of lanthanides, followed by a brief review of FRET theory and measurement, highlighting those areas where lanthanides differ from conventional probes. We then show a number of applications where LRET has enabled new types of systems to be studied: ion channels in living cells, the molecular motor myosin in vitro and in vivo, and the detection of binding events in high-throughput drug screening assays.

CHARACTERISTICS OF LUMINESCENT LANTHANIDE PROBES

Figure 1 shows four prototypical luminescent lanthanide probes. All contain an organic chromophore, which serves as an antenna or sensitizer, absorbing the excitation light and transferring the energy to the lanthanide ion. An antenna is necessary because of the inherently weak absorbance of the lanthanide (1 M^{-1} cm^{-1}, or 10^4–10^5 M^{-1} cm^{-1} smaller than conventional organic fluorophores.) The complexes also contain a chelate that serves several purposes, including binding

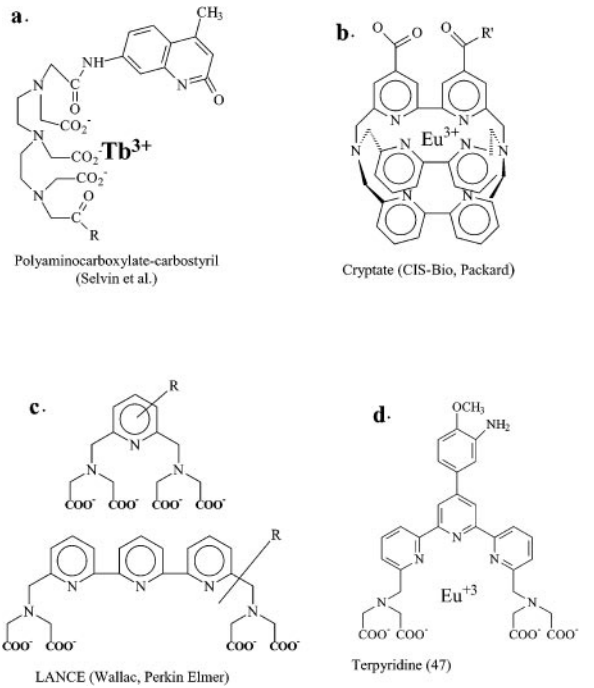

Figure 1 Structure of representative chelates.

the lanthanide tightly, shielding the lanthanide ion from the quenching effects of water, and acting as a scaffold for attachment of the antenna and a reactive group, the latter for coupling the chelate complex to biomolecules. In the cryptates, LANCE, and terpyridine probes (Figure 1*b–d*), the antenna is involved in binding the lanthanide; hence logically there is not a clear separation between chelate and antenna, whereas in the polyaminocarboxylate chelates such as DTPA-cs124 (Figure 1*a*) the DTPA chelate and cs124 antenna are distinct entities. All four sets of probes shown have been used as detection agents to replace either conventional fluorescent probes or radioactive probes [reviewed in (48)] where subpicomolar detection limits have been achieved (13, 21, 43, 47, 54, 64). They have also been used in resonance energy transfer application, which is the focus of this review (2, 6, 9, 17, 23, 25, 29, 34, 41–43, 55, 57, 62). The predominant application of the cryptates (commercialized by CIS-Bio International and Packard Instruments) and LANCE (commercialized by Wallac, now part of Perkin Elmer) have been in binding assays associated with high-throughput screening, whereas the primary application of the polyaminocarboxylate compounds have been in basic studies to measure conformational changes. However, all such chelates can be used in both applications. We focus on the polyaminocarboxylate chelates such as DTPA-cs124.

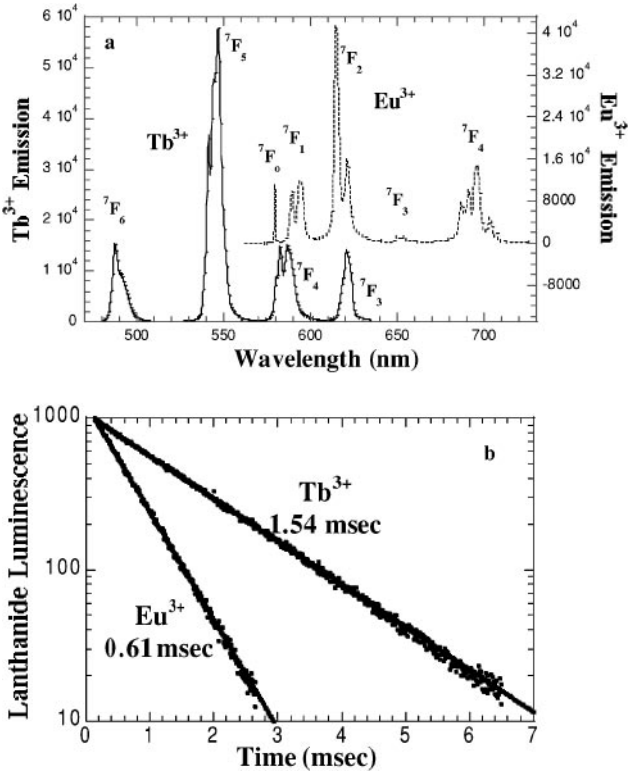

Figure 2 (*a*) Emission spectra and (*b*) lifetime of Tb^{3+}- and Eu^{3+}-DTPA-cs124.

Figure 2*a* shows the emission spectra and Figure 2*b* shows the excited-state lifetime characteristics of the DTPA-cs124 bound to either terbium or europium. These two are by far the most useful lanthanides. Dy and Sm are the only other two lanthanides that emit in the visible but with much weaker intensity (65). Excitation of the antenna is in the ultraviolet, typically utilizing the convenient nitrogen laser (337 nm), although flash lamps can also be used. Emission is in the green (Tb) and red (Eu). This large Stokes shift enables facile discrimination against excitation light. Eu and Tb emission are sharply spiked in wavelength, with long (msec) excited-state lifetimes. These attributes are important for resonance energy transfer applications (see below). The sharply spiked spectra occur because emission is atomic-like and the chelate shields the atom from broadening effects of the solvent. The long lifetime occurs because the electronic transitions involved in emission are formally forbidden by various selection rules (3). More specifically, emission arises from a 4f to 4f electronic transition and hence is parity forbidden; it also involves a high spin to high spin transition from an $S = 2$ state ($^5D_4$ for Tb^{3+}, $^5D_0$ for Eu^{3+}) to an $S = 3$ state (^7F_J, where $J = 0$–6). The high spin nature

of the transitions is why emission is formally neither fluorescence (singlet-to-singlet transition) nor phosphorescence (triplet-to-singlet transition). Despite the unusual nature of the atomic states, emission primarily arises from electric dipole transitions (3, 15). This is important because it is the same mechanism used by organic fluorophores. Hence, the electric field produced by a lanthanide donor and by an organic donor have the same distance dependence, i.e., they both decrease as $1/R^3$ for distances $\ll$ wavelength of light. Ultimately, this leads to the same distance dependence, R^{-6}, for resonance energy transfer measurements using either lanthanides or organic donors.

The emission quantum yield for terbium or europium in the chelates is also quite high (15). This is important because the efficiency of energy transfer is proportional to the donor quantum yield (Equations 3 and 5). By lanthanide quantum yield, Q_{Ln}, we mean the probability that the lanthanide will emit a photon given that the lanthanide is excited. This definition is similar to that used with conventional fluorophores, although there is a subtlety. Lanthanide excitation is a two-step process: The antenna absorbs a photon and then passes this energy onto the lanthanide with some finite probability ($\equiv Q_{transfer} \leq 1$) (Figure 3). The lanthanide then emits with some probability, i.e., the quantum yield mentioned above, Q_{Ln}. The overall probability that the lanthanide will emit a photon (Q_{total}), given that an excitation photon was absorbed by the complex (antenna), is

$$Q_{total} = Q_{Ln} \times Q_{transfer}. \quad (1)$$

For organic fluorophores, $Q_{transfer} \equiv 1$ and hence $Q_{total} = Q_{Ln}$. For Tb^{3+} and Eu^{3+} in polyaminocarboxylate chelates such as in Figure 1*a*, $Q_{transfer} = 0.4$–0.75 and $Q_{total} = 0.1$–0.4 (64). In any case, the efficiency of energy transfer (related to R_o, the distance at which half the donor's energy is transferred to the acceptor, e.g., Equation 5) is proportional to Q_{Ln}, and Q_{total} is only relevant in that it affects the total brightness of the sample.

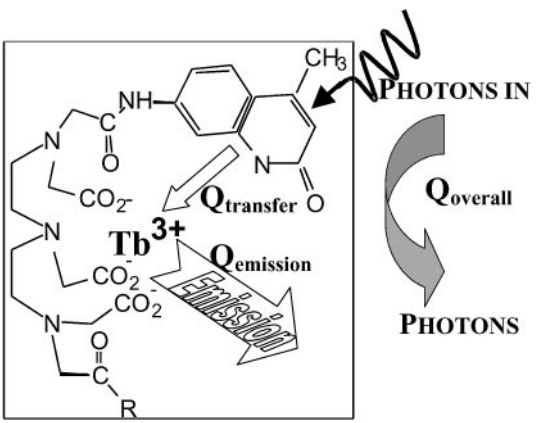

Figure 3 Definition of quantum yields.

In order for the lanthanides to be useful in bioassays, the chelates must have a reactive group for attachment to biomolecules. Fortunately, the standard reactive groups can be coupled to the chelates: Amine-reactive groups such as isothiocyanates (36) and thiol-reactive groups such as maleimides, bromoacetamides, and pyridyl dithio (8) have been made for the polyaminocarboxylate chelates. The same or similar reactive groups have been made for the LANCE (58) and cryptates (see also www.perkinelmer.com). The reactive groups can, however, lead to more complicated photophysics in that they can interact with the antenna molecules or adopt multiple conformations, leading to multi-exponential lanthanide decays, particularly with terbium (8).

LANTHANIDE-BASED RESONANCE ENERGY TRANSFER

In resonance energy transfer experiments, using lanthanides as donors to transfer energy to organic-based acceptors leads to many technical advantages compared to using all-organic dyes. Because lanthanide emission is not formally fluorescence, we call the technique lanthanide- or luminescence-resonancy energy transfer (LRET), as opposed to FRET, for which we mean energy transfer using organic dyes. Despite the differences, the mechanism of energy transfer is the same in FRET and LRET; hence the underlying theory and formulas can be used, subject to careful interpretation of various terms. Here we quickly review the theory and measurement of FRET and highlight those parts relevant or different in LRET.

FRET and its derivative, LRET, are techniques for measuring the distance between two points that are separated by approximately 15–100 Å. The techniques are valuable because measurements can be made under physiological (or other) conditions with near-Angstrom resolution and with the exquisite sensitivity of fluorescence measurements. In FRET or LRET, a donor fluorophore is excited and transfers energy to an acceptor fluorophore in a distant-dependent fashion. The classical physics view of this process is that the donor, after being excited, produces an oscillating electric dipole field that decays with distance (R). At distances less than the wavelength of light (λ), the electric field predominantly drops off as R^{-3}. (For $R \gg \lambda$, $E \alpha R^{-1}$, which is simply the electric part of the propagating field that is the emitted photons.) An acceptor, if nearby and containing energy levels corresponding to the frequencies of the oscillating electric field, can interact with this field and become excited, taking energy. The probability of the acceptor being excited depends on the square of the electric field strength and hence decays as R^{-6} for $R \ll \lambda$, the relevant distance scale in FRET/LRET ($\lambda \approx 500$ nm). Energy transfer also depends on how well the acceptor energy levels match the frequencies of the donor (the so-called spectral overlap term, e.g., Equation 6). Finally, energy transfer may also depend on the orientation of the donor and acceptor (the "κ^2" term, e.g., Equations 5 and 7) because the electric field of the donor may be polarized and anisotropic.

The efficiency of energy transfer, E, is defined as the probability that an excited donor will return to the ground state by giving its energy to an acceptor. This can

be written as

$$E = k_{et}/(k_{et} + k_{nd}) = 1/(1 + k_{nd}/k_{et}) = 1/(1 + 1/k_{et}\tau_D), \quad (2)$$

where k_{et} is the rate of energy transfer and is distant-dependent, and k_{nd} is the rate of all other donor decay processes, such as the radiative and nonradiative rates of donor decay. These latter processes clearly do not depend on the donor-acceptor distances. The donor lifetime in absence of acceptor is τ_D. Note that E depends on the ratio k_{et} to other processes but does not depend on the absolute donor lifetime. In FRET, donor rates (or lifetimes) and energy transfer rates are in the nanosecond range, whereas in LRET they are in the millisecond range; both can yield similar values of E. As a side point, if the distance between the probes changes slowly on the FRET timescale, but quickly on the LRET timescale, the two techniques can give dramatically different energy transfer efficiencies. Indeed, one signature of such dynamics is if LRET gives a much higher E than FRET (7).

Because the rate of energy transfer depends on the R^{-6} distance between donor and acceptor, Equation 2 can be rewritten as

$$E = 1/\left(1 + R^6/R_o^6\right) \quad (3)$$

or, rearranging,

$$R = R_o(1/E - 1)^{1/6}, \quad (4)$$

where R_o is a constant depending on the spectral properties of the dyes as well as their relative orientation, and it is the distance at which E = 0.5. Consequently, if R_o can be determined or calculated and E measured spectroscopically, then FRET/LRET can be used as a spectroscopic ruler to determine distances (56).

R_o is usually calculated from the spectral properties of donor and acceptor (5):

$$R_o = 0.21\left(Jq_D n^{-4}\kappa^2\right)^{1/6} \text{ (in Angstroms)} \quad (5)$$

$$J = \int \varepsilon_A(\lambda)\, f_D(\lambda)\lambda^4 d\lambda \Big/ \int f_D(\lambda)\, d\lambda \text{ in } \underline{M}^{-1}\,\text{cm}^{-1}\,\text{nm}^4, \quad (6)$$

where J is the normalized spectral overlap of the donor emission (f_D) and acceptor absorption (ε_A in units of $\underline{M}^{-1}$ cm^{-1}, where $\underline{M}$ is units of Moles/liter), q_D is the quantum efficiency (or quantum yield) for donor emission in the absence of acceptor (q_D = number of photons emitted divided by number of photons absorbed), n is the index of refraction (1.33 for water; 1.29 for many organic molecules), and κ^2 is a geometric factor related to the relative orientation of the transition dipoles of the donor and acceptor and their relative orientation in space. Note that for LRET, q_D in Equation 5 is Q_{Ln} and not Q_{total} (Equation 1). This is because Q_{Ln}, not Q_{total}, determined the strength of the donor's electric field.

The orientation term, κ^2, in R_o, is often a source of uncertainty in FRET measurements. It is defined as

$$\kappa^2 = (\cos\theta_{DA} - 3\cos\theta_D \cos\theta_A)^2, \quad (7)$$

where θ_{DA} is the angle between the donor and acceptor transition dipole moments, and θ_D (θ_A) is the angle between the donor (acceptor) transition dipole moment and the R vector joining the two dyes. By measuring the polarization of donor and acceptor emission, constraints on these angles can often be imposed, reducing—although usually not completely eliminating—the uncertainty in κ^2. κ^2 ranges from 0 if all angles are 90 degrees to 4 if all angles are zero degrees, and it equals 2/3 if the donor and acceptor rapidly and completely rotate during the donor excited-state lifetime (14). If the donor is unpolarized, as is the case for terbium and usually europium (J. G. Reifenberger, G. E. Snyder & P. R. Selvin, manuscript in preparation), and the acceptor is completely rigid and either parallel ($\kappa^2 = 2/3$) or perpendicular ($\kappa^2 = 1/3$) to the radius vector, then $1/3 < \kappa^2 < 2/3$. This limits the worst case error in R_o to -11% $+12\%$ if one simply assumes $\kappa^2 = 2/3$. Furthermore, because the lanthanides have millisecond lifetimes, the acceptor will likely rotate during this time, making κ^2 very close to 2/3. Hence, the error in distances measured via LRET due to the orientation factor is essentially negligible. This in turn makes the distance determination via LRET generally more accurate than FRET because the orientation factor in FRET is often poorly known.

Finally, R_o is also proportional to J, the spectral overlap. The lanthanides have highly spiked emission spectra in regions where several excellent dyes absorb (Figure 2*a*), e.g., the Tb^{3+} 490 nm emission peak overlaps well with fluorescein, green fluorescent protein, and Alexa 488 absorption; the Tb^{3+} 546 nm peak overlaps with Cy3, tetramethylrhodamine, Alexa 546, and R-phycoerythrin absorption; the Eu 617 nm peak overlaps with Cy5, Alexa 633, and allophycocyanin absorption. Consequently, J for LRET can be unusually large. When combined with a high Q_{Ln}, the R_o in LRET can also be quite large (Table 1).

Measuring E

In Figure 4, an energy transfer experiment between a terbium-labeled DNA and a rhodamine-labeled DNA complement is shown (52). This example highlights various ways of measuring energy transfer. In FRET and LRET there are several ways of measuring E: a reduction in donor intensity in the presence of acceptor because some of the energy is going to the acceptor instead of into donor emission, by a decrease in donor excited-state lifetime because energy transfer to the acceptor is an additional relaxation pathway of the donor's excited state, or by an increase in acceptor fluorescence because the acceptor is receiving energy from the donor and converting this energy into acceptor fluorescence. In LRET, E can also be measured via the sensitized-emission lifetime (see below). In FRET (but not LRET) E can also be measured by an increase in the photostability of the donor in the presence of acceptor because energy transfer to the acceptor decreases the donor's excited-state lifetime, and photobleaching is generally proportional to the amount of time the dye spends in its excited state. Finally FRET and potentially LRET can be measured by an increase in donor intensity following photodestruction of the acceptor (30).

TABLE 1 J-values and R_o for lanthanide chelates and organic dyes

Donor-acceptor pairs*	J-value (M^{-1} cm^{-1} nm^4)	R_o (Å)
Terbium to fluorescein (bound to DNA) (ε_{max} = 75k @ 492 nm)	9.23×10^{14}	45.0
Terbium to eGFP (free) (ε_{max} = 55k @ 488 nm)	7.14×10^{14}	43.1
Terbium to TMR (bound to DNA) (ε_{max} = 100k @ 557 nm)	3.80×10^{15}	57.0
Terbium to Cy3 (free) (ε_{max} = 150k @ 552 nm)	5.82×10^{15}	61.2
Terbium to R phycoerythrin pH 7.5 (free) (ε_{max} = 1960k @ 566 nm)	9.60×10^{16}	97.5
Europium to Cy5 (bound to myosin) (ε_{max} = 249k @ 650 nm)	8.89×10^{15}	55.2
Europium to allophycocyanin pH 7.5 (free) (ε_{max} = 700k @ 652 nm)	4.01×10^{16}	71.0

*J and R_o calculated for terbium and europium using corrected emission spectra and quantum yields for lanthanide bound to DTPA-cs124 in aqueous solutions ($q_{Tb} = 0.48$; $q_{Eu} = 0.17$). J and R_o in D_2O and in other chelates with same emission spectra can be determined by multiplying by the appropriate quantum yields, found in (64). Other constants: n = 1.33; $\kappa^2 = 2/3$. The emission spectra of Tb^{3+} and Eu^{3+} are insensitive to attachment to biomolecules, although the absorption spectra of the acceptor dye can be somewhat sensitive to attachment. Absorption spectra of R phycoerythrin and allophycocyanin are from Molecular Probes Inc., and Cy-3 from Amersham.

The efficiency of energy transfer (E) is then

$$E = \left(1 - I_{D_A}/I_D\right) = 1 - \tau_{D_A}/\tau_D = 1 - \tau_{A_D}/\tau_D = 1 - \tau_D^{bl}/\tau_{D_A}^{bl}, \qquad (8)$$

where I_{D_A}, τ_{D_A}, and $\tau_{D_A}^{bl}$ are the donor's intensity, excited-state lifetime, and photobleaching time constant in the presence of acceptor, and I_D, τ_D, and τ_D^{bl} are the same parameters in the absence of acceptor. τ_{A_D} is the lifetime of the sensitized emission of acceptor (discussed further below).

Although using absolute intensities, I_{D_A}, I_D, is conceptually straightforward, it involves matching concentrations of two different samples and hence is prone to titration errors. Lifetime measurements avoid this problem and also resolve multiple species with different E's. Figure 4*b* shows a single-exponential donor-only lifetime that is reduced upon hybridization with an acceptor-containing DNA strand. Starting with a single-exponential donor-only lifetime is not essential but significantly simplifies the analysis of complex donor-acceptor mixtures. Titrating in with substoichiometric amounts of acceptor strand leads to two populations and hence a bi-exponential donor decay: a donor-only unhybridized strand (τ_{D_A} = 2.1 msec) and donor-acceptor double-stranded DNA ($\tau_{D_A} = 330\ \mu$sec). The amount of energy in the donor-acceptor pair can be calculated in Equation 8 using the

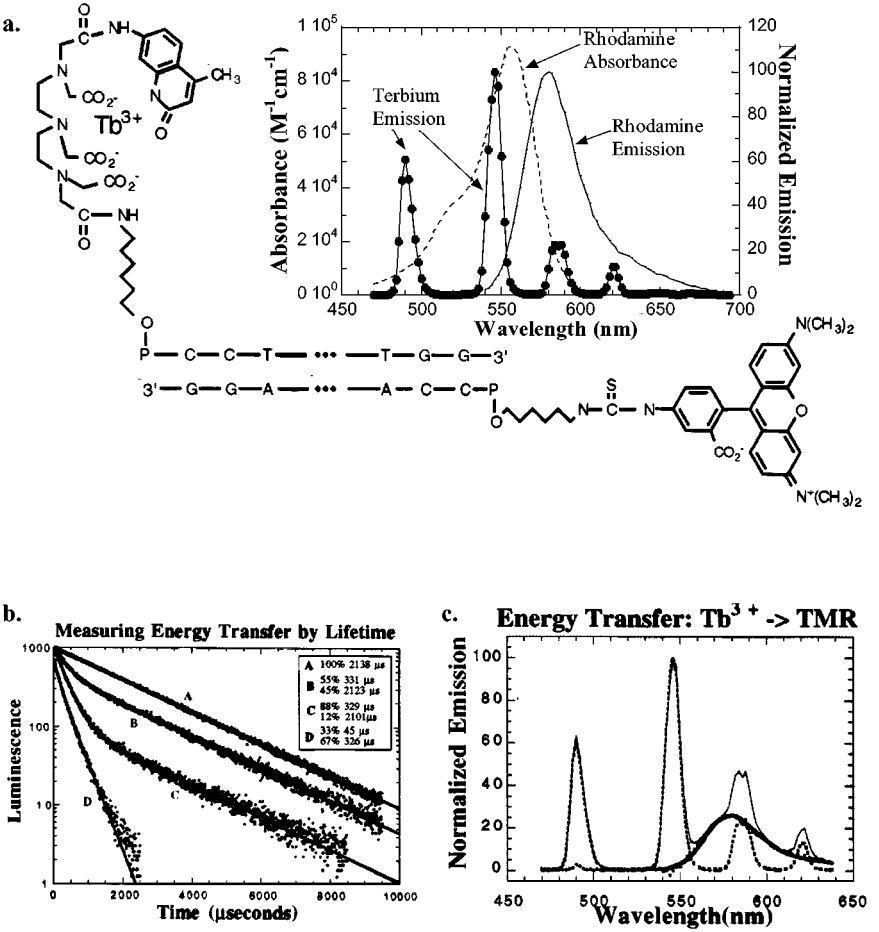

Figure 4 (*a*) DNA hybridization and model system for LRET. (*b*) Lifetime data. (*c*) Spectral data. [Figure adapted from (52)].

330-μsec lifetime and the donor-only lifetime of a terbium DNA hybridized to an unlabeled complementary DNA, which is 2.8 msec (data not shown). The relative populations of the two species can be determined by their pre-exponential amplitudes. Titrating in more acceptor strand increases the amplitude of the short time component but leaves its lifetime unchanged, as expected.

In LRET, E can also be measured by measuring the lifetime of the sensitized emission of acceptor (Figure 4*b*, *curve D*). The donor is excited by a pulse of light, the direct acceptor emission decays in nanoseconds, and any acceptor emission after this initial delay is therefore due only to energy transfer received by the acceptor from the long-lived donor. Its lifetime, τ_{A_D}, will follow the donor's lifetime, τ_{D_A}. Importantly, τ_{A_D} can be measured without contaminating background from either direct acceptor fluorescence via temporal discrimination or from donor

emission via spectral discrimination. The latter is possible because the donor is sharply spiked in emission spectra, including regions where the donor is dark yet where the acceptor fluoresces. For example terbium is dark around 520 nm and 570 nm, where fluorescein and tetramethylrhodamine emit, respectively. Consequently, the temporal decay of the acceptor-sensitized emission can be measured with no background, from either donor leakage or direct acceptor leakage. This sensitized-emission lifetime is a powerful advantage of LRET because it only arises from donor-acceptor pairs. In Figure 4*b*, *curve D*, the sensitized-emisison lifetime closely matches the short component of the donor lifetime; however, it does not have contamination from the donor-only DNA strands. The pre-exponential amplitudes of a sensitized-emission decay correspond to the population of excited acceptors. Hence, in a multi-exponential decay corresponding to a distribution of donor-acceptor pairs, the pre-exponential terms are the product of the individual energy transfer efficiencies and their populations (24). This is in contrast to the donor decay, where the amplitudes are just proportional to populations.

E can also be determined by measuring the increase in fluorescence of the acceptor due to energy transfer and comparing this to the residual donor emission,

$$E = \left[I_{A_D}/q_A\right]/\left[I_{D_A}/q_D + I_{A_D}/q_A\right], \quad (9)$$

where I_{D_A} is the integrated area under the donor-emission curve in the presence of acceptor, I_{A_D} is the integrated area of the sensitized emission of the acceptor (i.e., not including the fluorescence due to direct excitation of the acceptor by the exciting light source), and q_i is the quantum yield for donor or acceptor. The integrated areas are determined by curve-fitting the spectrum to the sum of a donor-only and acceptor-only spectra. Qualitatively, this equation says that energy transfer takes area under the donor-emission curve to area under the acceptor curve. Because E is defined in terms of excitations, not emissions, these areas are normalized by their quantum yields, which is just the ratio of emissions to excitations. More specifically, the numerator is the number of excitations of the acceptor due to energy transfer. The left-hand term of the denominator is the number of donor excitations that do not lead to energy transfer. The right-hand term is the donor excitations that do lead to energy transfer, i.e., acceptor excitation.

Figure 4*c* shows the time-delayed emission spectra of the donor and donor-acceptor complex (corresponding to *curve C* in Figure 4*b*), which can be used to determine the two intensities in Equation 9. The donor-acceptor sample is excited using a short excitation pulse, and emission is detected after a few tens of microseconds delay. This procedure eliminates all prompt fluorescence of the acceptor. It also eliminates any contribution from acceptor-only species, if present, as well as any direct fluorescence from the antenna, both of which have nanosecond lifetimes. The donor-acceptor spectrum is then fit to the sum of a donor and acceptor spectra, with I_{D_A} being the area due to donor emission and I_{A_D} equal to the area under the acceptor emission. Note that the absolute concentrations of the donor-only species, the acceptor-only species, and the donor-acceptor species are irrelevant. In practice, the curve-fitting is done as follows: The donor-only spectra and donor-acceptor spectra are normalized at the 490-nm peak, or at any point where

there is no acceptor fluorescence. The donor-only curve is then subtracted from the donor-acceptor spectra, and the difference is the sensitized-emission curve, with area I_{A_D}. This should have the same shape as an acceptor-only emission spectra. I_{D_A} is simply the area under the donor-curve. (Although we always take a donor-only spectra as a control (*dashed line*, Figure 4*c*), the spectral shape of Tb-DTPA-cs124 does not change under any condition tested; hence a donor-only spectrum taken once is likely to remain unchanged.)

There are two additional points needed to properly use Equation 9. First, the emission spectra must be corrected for wavelength sensitivity of the detector. This is done via conventional means, using an emission source (standard lamp or a dye) whose emission spectra are known (35). Second, the donor and acceptor quantum yields must be measured. Fortunately, we have recently determined the quantum yield of Tb^{3+} and Eu^{3+} in free polyaminocarboxylate chelates (64). The quantum yield of lanthanide chelates bound to biomolecules can then simply be determined by comparing lifetimes to the free chelates. Acceptor quantum yields can be measured by conventional means: intensity or lifetime comparison to standards such as fluorescein [QY = 0.93 in 1 N NaOH (61)], or tetramethylrhodamine [QY = 0.58 in 10-mM Na-phosphate buffer, pH 7.46, 80-mM NaCl, room temperature (60)], or sulforhodamine 101 [QY = 1, lifetime = 4.36 nsec, in methanol (33)].

The importance of Equation 9 is that it allows accurate measurement of relatively small amounts of energy transfer (distances $>R_o$). It is also interesting to note, although not widely appreciated, that by combining equations 4, 5, and 9, the calculated distance depends only on the acceptor quantum yield and not on the donor quantum yield:

$$R = C\left[I_{D_A} q_A / I_{A_D}\right]^{1/6}, \quad (10)$$

where C is simply all the constants in R_o except q_D. Finally, Equations 9 and 10 can also be used in conventional FRET, but here the direct excitation of acceptor must first be subtracted off (11).

In summary, the advantages of LRET include large signals (big R_os) with low backgrounds, enabling long distances to be determined with little uncertainty due to orientation factors. Energy transfer can be measured accurately because absolute concentrations do not matter via spectral measurements, and the μsec-msec lifetimes can be measured accurately via temporal measurements. The extent of donor and acceptor incorporation has only a minor effect on LRET measurements because, via sensitized-emission lifetime measurements, donor-only and acceptor-only species do not contribute contaminating backgrounds. This lack of sensitivity to incomplete labeling is particularly important in cellular applications, where 100% labeling and purification cannot usually be achieved.

Instrumentation

The instrumentation used to perform LRET is relatively simple, although slightly more complex than conventational steady-state fluorimeters. The general requirements are a pulsed UV excitation source and time-resolved detection. The pulsed

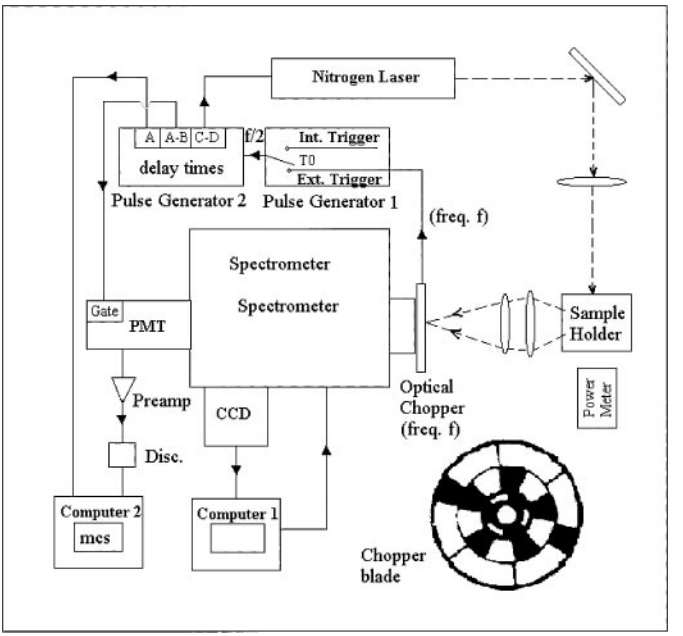

Figure 5 LRET instrumentation. A pulsed nitrogen laser excites the lanthanide sample, and emission is collected by a mechanically chopped spectrometer and CCD for time-delayed spectral measurements, or a spectrometer and electronically gated PMT for excited-state lifetime measurements. [Figure from (63)].

excitation source is usually a nitrogen laser (337 nm, 5-nsec pulse-width typical, 20–50-Hz repetition rate). For lifetime measurements, a photomultiplier tube with suitable color filters and counting electronics is used. For time-delayed spectra, a spectrometer, typically utilizing diffraction gratings, and either a time-gated photomultiplier tube or preferably a CCD, gated either electronically or with a mechanical chopper, are used. A schematic of the instrument built in my laboratory is shown in Figure 5 and details are given elsewhere (63, 64).

APPLICATIONS

The technical advantages of LRET open up many applications. We highlight a few representative examples from my lab, as well as from others.

Ion Channels

We have used LRET to measure conformational changes in the Shaker potassium ion channel, a voltage-gated channel involved in nerve impulses. In many ways this is an extremely demanding use of LRET. The measurement is on a living cell (*Xenopus* oocytes); hence purification of completely labeled donor-acceptor

species is not possible. Indeed, a heterogeneous mixture of labeled proteins exists, all in the presence of nonspecific labeling to other membrane components. Furthermore, two distances are expected to exist (see below) and the distance changes (as a function of voltage—see below) are quite small—a few Ångstroms. The technical advantages of LRET help overcome these difficulties.

The channel is a transmembrane protein, consisting of four identical subunits (Figure 6*a,b*) with fourfold symmetry. Each subunit contains six transmembrane-spanning segments, S1–S6 (Figure 6*c*). A pore, or channel, is formed at the intersection of the four subunits, which is opened or closed, i.e., gated, depending on the voltage across the cell membrane. At the resting transmembrane potential of approximately −60 mV, the pore is closed. Upon depolarization to approximately 0 mV, the protein undergoes a conformational change that ultimately leads to an opening of the pore, allowing potassium ions to flow from the inside to outside of the cell, down its electrochemical gradient. The flow of potassium ions along with the flow of sodium ions through analogous sodium channel are the electrical currents that form nerve impulses.

One of the transmembrane segments, S4, is known as the "voltage sensor" and contains seven positively charged amino acids. These charges feel a force due to the transmembrane potential or electric field and are likely to move in response to changes in these fields. A second segment, S2, also contains some positively charged residues and likely plays a secondary role in voltage sensing as well.

Fundamental questions remain regarding how the channel senses and responds to voltage. What is the structure of the S4, e.g., is it an alpha helix? How does it sit in the membrane—perpendicular to the membrane or tilted at an angle? How does the S4 move in response to voltage changes? Does it move like a plunger, e.g., moving up and down, perpendicular, or at some angle to the membrane? Or does it rotate like a knob, perhaps with little transmembrane motion? Or is the movement some combination, perhaps like a corkscrew rotating and translating? And finally, how is the motion of S4 coupled to the pore region such that a motion of S4 leads to opening and closing of the pore?

Cysteine-scanning mutagenesis is the most common method for detecting conformational changes in ion channels. The idea is to look at changes in accessibility of engineered cysteines to external-labeling reagents. Labeling of reagents can be detected if they have an effect on ionic or gating currents. (Ionic current is the flow of potassium ions through the pore; gating currents are transient currents created by the movement of the charged residues in the protein, mostly on S4 and S2.) This method, however, is quite indirect since changes in labeling efficiency can be due to several factors and not all sites lead to changes in gating properties. Isacoff et al. (39), and shortly thereafter, Bezanilla and colleagues (5a), introduced the use of fluorescent-labeling reagents to detect conformational changes. Here a fluorophore was attached to an engineered cysteine in S4 and changes in fluorescence with changes in voltage were measured. These fluorescence changes were interpreted as arising from changes in the local environment around the fluorophore, e.g., from a more hydrophic or membrane-like environment to a more water-like

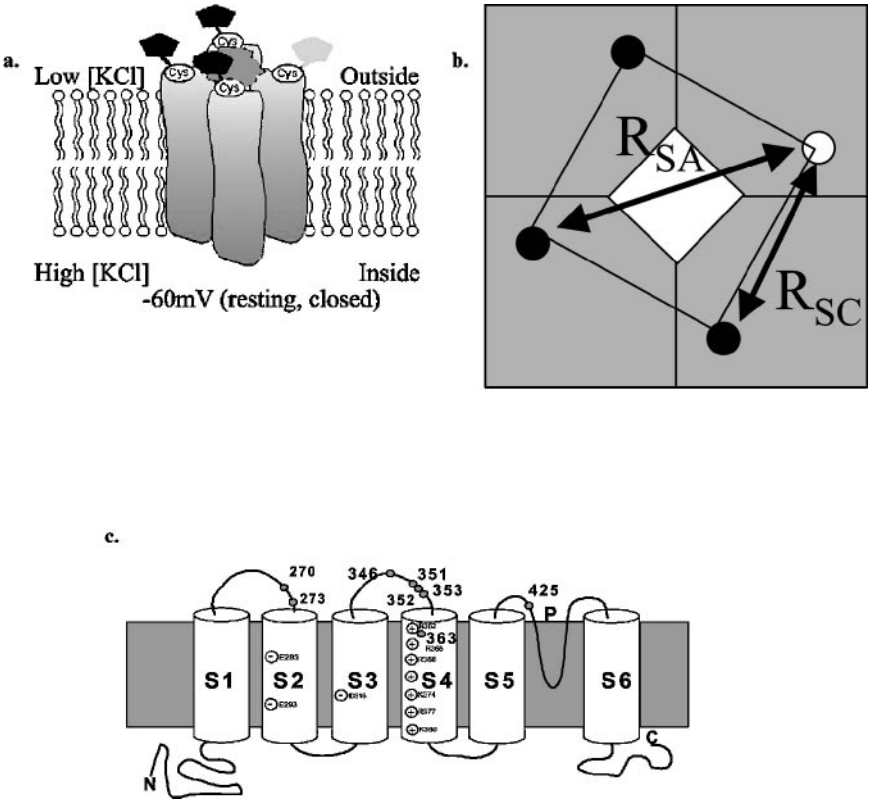

Figure 6 Structure of Shaker potassium ion channel and labeling scheme. (*a*) Side view, (*b*) top view, (*c*) substructure. The channel consists of a central pore (*dark gray* in 6*a*) surrounded by four identical subunits. Each subunit consists of six transmembrane domains (6*c*) and is labeled with either a donor (*black*, 6*a*,*b*), or acceptor (*light gray*, 6*a*; *white*, 6*b*). Labeling is done such that there are 3 donors (*black*) and only one acceptor (*white*) per channel. Specific labeling is achieved by introducing a unique cysteine in the S3-S4 linker, near S4, which is the voltage sensor.

environment (39). This led Isacoff et al. to postulate a translational, transmembrane movement of the S4, bringing fluorophores buried inside the membrane to a more extracellular region. However, changes in fluorescence are also an indirect measurement of conformational changes. FRET, or LRET, is a much more direct measure (51). In more recent work the Isacoff group (18) used FRET to measure S4 motion, and the Bezanilla and Selvin groups used LRET (6). Both concluded there was a rotation of S4, although based on the LRET methodology, Bezanilla and Selvin concluded there was not a large transmembrane movement, whereas the Isacoff group argued such a motion may exist. A detailed comparison of the two experiments has been published (27). Here we review the LRET experiment.

For labeling the channel, a single engineered cysteine was introduced at various positions in the S3-S4 linker, near the top of the S4. Each channel therefore contains four cysteines, one on each subunit. Conveniently, the Shaker channel does not contain native cysteines that are reactive to extracellularly applied probes. Channels were expressed in *Xenopus* oocytes and labeled with a mixture of donor and acceptor probes, the donor in excess to ensure that most channels contain at most only one acceptor. Under this condition, two different donor-acceptor distances are expected (Figure 6*b*). A donor sees an acceptor on a contiguous subunit (distance R_{SC}) or on a subunit across the pore (distance R_{SA}). To measure these distances, we focused on measuring the sensitized-emission lifetime. This has the great advantage that those channels containing all donors—the majority of channels—do not contribute signal and can be ignored. (Those containing all acceptors can also be ignored, although this is a small fraction of the channels.) We therefore expect the sensitized-emission lifetime to be bi-exponential, with the shorter lifetime corresponding to the greater E and shorter distance. Figure 7*a* shows this behavior for a probe labeled at position 346. The two distances are in excellent agreement with the expected Pythagorean relationship. By placing probes at various positions, ranging from 363 near the top of S4 to 346 near the middle of the S3-S4 linker, we found that the intersubunit distances decreased. This implies that S3-S4 (and perhaps S4) is tilted toward the pore as one moves in the extracellular direction.

In FRET, and to a certain extent in LRET, absolute distances are always more difficult to measure than relative distances. However, to check whether our absolute distances were reasonable, we measured distances between residues 425. This residue is found in the crystal structure of the KcsA channel, a (nonvoltage-gated) prokaryotic analog of Shaker containing two transmembranes per subunit, analogous to S5 and S6. We found $R_{SA} = 30$ Å, in excellent agreement with the $C_\alpha - C_\alpha$ 29 Å distance in the crystal structure. Furthermore, after publication of our LRET results, other workers measured distances using "tethered linkers" and found excellent agreement in absolute distances to our results (1). This is in sharp contrast to the FRET results (18), which yielded much larger absolute distances. The latter probably occurred because of uncertainties in donor quantum yields and possibly because of the κ^2 factor.

Next we measured intersubunit distances as a function of voltage. Changes in lifetime and hence distances between site 346 near S4 are shown in Figure 7*b*. Figure 7*c* shows a plot of R_{SC} versus voltage, superimposed on gating charge movement. Strikingly, the changes in distance at 346 strongly mirror gating charge movement, implying that the distances we measure at 346 are related to the charge movement in S4 and functioning of the channel. By modeling the distance versus voltage curve, we concluded that a large transmembrane motion did not occur (6). Furthermore, small but statistically significant changes in distance were found at positions 350, 351, and 352, where 351 moved farther apart, 350 remained unchanged, and 352 moved closer together (Figure 8*a*). The simplest model to account for this nonmonotonic behavior is to postulate that the S3-S4 linker is helical and undergoes a rotation about its long axis (Figure 8*b*). Because

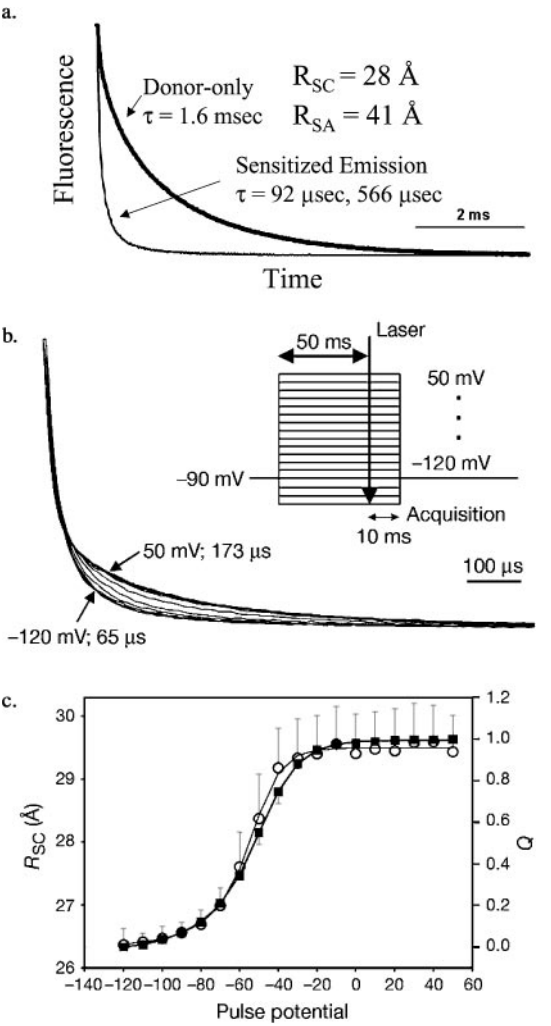

Figure 7 (*a*) Biexponential sensitized emission, corresponding to two donor-acceptor distances, corresponding to distances between subunits across the channel and neighboring subunits. (*b*) Voltage-dependent changes in sensitized emission arising from movement of S346C in the voltage-sensing region of Shaker potassium channel. (*c*) Changes in distance between S346 and amount of charge in S4 moved across membrane potential. The changes in distance closely mirror the charge movement in S4. [Figures from (6)].

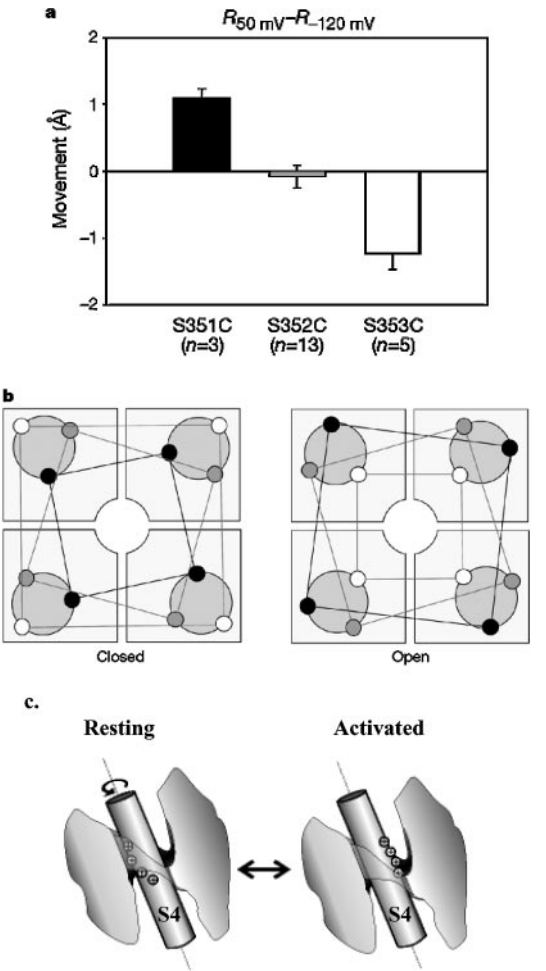

Figure 8 Changes in distance between sites 351–353. These data can be explained by a rotation of a helical segment of the ion channel (*b*), leading to a model where the voltage sensor, S4, may undergo a rotation in response to voltage (*c*). [Adapted from (6, 18)].

the S3-S4 linker distance changes are coupled closely to the charge movement of S4, S4 may also undergo a rotation (Figure 8*c*) in response to voltage. That such small distance changes can be measured is a tribute to the power of LRET, although interpretation of such small distance changes must be made with caution. Interestingly, a rotation in ligand-gated ion channels (26, 28) and a transporter (37) has recently been measured, which suggests that helix rotation may be a general feature of membrane channels.

APPLICATION 2: CONFORMATIONAL CHANGES IN A RNA POLYMERASE SUBUNIT UPON DNA BINDING

Protein-Induced DNA Bends

The Heyduk lab has been active in using LRET to study DNA-protein interactions. In one of their earlier works they used LRET to measure protein-induced DNA bending (25), which is involved in the packaging and regulation of DNA. They used LRET, for example, to measure the bending of a 30mer double-stranded DNA oligomer by a class of proteins known as high-mobility group (HMG) proteins. The DNA was 5′-labeled with europium and Cy5, and distances out to 100 Å were measured with energy transfer efficiencies of less than 3%. This was possible because of LRET's capability to accurately determine lifetimes, especially when the donor is single exponential. The Ebright lab has also recently applied LRET using a terbium chelate to measure 100 Å distances in DNA complexes bent by the CAP protein (32).

Recently, Heyduk and coworkers have used LRET to study conformational changes in RNA polymerase upon binding to DNA and transcription initiation in prokaryotes (4, 23). The first step in transcription initiation in prokaryotes involves recognition of promoter DNA sequence by a multisubunit enzyme RNA polymerase [reviewed in (20)]. One of the subunits, σ^{70}, is involved in the initial recognition of the promoter DNA via direct protein-DNA contacts separated by $\sim$17 base pairs. σ^{70} exists in the cell in two major forms: free and in complex with the remaining RNA polymerase subunits (core polymerase). However, only σ^{70} in complex with the core RNA polymerase is able to specifically recognize promoter DNA, whereas the free σ^{70} does not bind to promoter DNA. Thus, the promoter recognition capabilities of σ^{70} are allosterically regulated by an interaction of σ^{70} with the core polymerase.

LRET experiments were used to investigate the nature of the regulation of σ^{70} promoter DNA-binding activity (4). The idea was to look for conformational differences in σ^{70} in the bound and free form that might affect its DNA-recognition ability. The specific incorporation of the donor (DTPA-Eu-DTPA-AMCA-maleimide) (22) and the acceptor (Cy5 maleimide) into selected domains of σ^{70} was achieved by preparing a set of σ^{70} mutants with pairs of unique reactive cysteine residues engineered into the desired locations. Since both donor and acceptor were thiol-reactive, and both labeling sites were cysteine residues, a mixture of donor-donor, donor-acceptor, and acceptor-acceptor labeling resulted. However, by using LRET, the sensitized emission arising from only the donor-acceptor complex could be measured. Good quality determinations of τ_{ad} were possible in this case even though the donor-acceptor species constituted only approximately 25% of the mixture. This is possible because the donor-only and acceptor-only species do not contribute background signals. Representative LRET data are shown in Figure 9. It would be difficult to perform these measurements with FRET utilizing classical fluorescence probes.

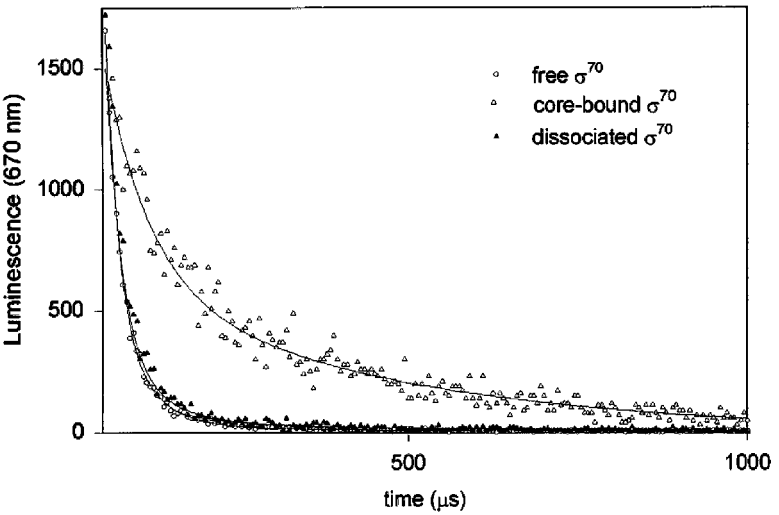

Figure 9 The effect of core RNA polymerase on σ^{70} measured by sensitized-emission lifetime. Thiol-reactive Eu donor and Cy5 acceptor were labeled at positions A59C to R596C in σ^{70}, and sensitized emission of free and core-bound σ^{70} was measured. The increase in sensitized-emission lifetime upon core binding indicates less energy transfer and an increase in distance between these sites. [Figure from Figure 3*D* of (4)].

Comparison of distances measured for the free σ^{70} and the core-bound σ^{70} revealed that most distances were significantly increased upon binding of σ^{70} to the core polymerase. (DNA was not present in these experiments because σ^{70} binding to the core polymerase is not DNA dependent.) One of the distances measured, between residues 442 and 366, allowed a direct comparison between a distance measured by LRET in solution and a distance between the same residues measured in the crystal structure (38). Excellent agreement between these distances was found—35 Å in the crystal structure versus 38 Å measured via LRET—providing a further validation of LRET results. In total six distances between four sites in the σ^{70} protein were measured, making it possible to build three-dimensional models of the architecture of σ^{70} protein domains in free and core-bound protein.

In conclusion, these DNA and DNA-protein studies were greatly facilitated by LRET's ability to measure long distances and under labeling conditions where only a small fraction of the protein contained both donor and acceptor labels.

APPLICATION 3: MEASURING MOLECULAR INTERACTIONS IN A CELL

Douglas Root has used LRET to study the interaction of the proteins dystrophin and actin in the muscle cell (46). Dystrophin is present in the inner muscle cell membrane and is believed to stabilize muscle fibers by binding to actin filaments

and ultimately creating a bridge to the extracellular matrix. This model requires the direct association (close proximity) between dystrophin and actin, and there is significant in vitro evidence for this. However, because some proteins bind in vitro but not in vivo, Root asked the question whether this association is present in the muscle cell.

Root used thin (20 μM) tissue sections of muscle cells and specifically labeled dystrophin with monoclonal antibodies labeled with Tb-DTPA-cs124. Actin was stained with phalloidin-tetramethylrhodamine. This pair was reported to have a R_o of 59 Å, although 56 Å is probably more accurate (e.g., Table 1, which lists values for R_os) (64). In any case, a relatively large R_o is necessary to get reasonable energy transfer because of the large size of antibodies ($\approx$100 Å). If the donor antibody on dystrophin is in close proximity, roughly within R_o, of the acceptor-labeled actin, then energy transfer should be observed. If the distance is large ($\gg R_o$), then no energy transfer is expected.

In fixed tissues donor intensity decreased 40% (in unfixed tissue 60%) in the presence of acceptor, indicating significant energy transfer and therefore a close association between anti-dystrophin antibodies and actin (Figure 10). Sensitized emission (using delayed detection to eliminate prompt acceptor fluorescence) was also observed. In addition, Root measured donor and sensitized-emission lifetime measurements (fitting to a single exponential) and found that the sensitized-emission lifetime (at 568 nm) was similar but somewhat shorter than the donor-lifetime (at 547 nm) [data not presented here, but see (46)]. This indicates that most, but not all, of the anti-dystrophin antibodies had an acceptor nearby. (A comparison of donor lifetime to sensitized-emission lifetime gives information about the

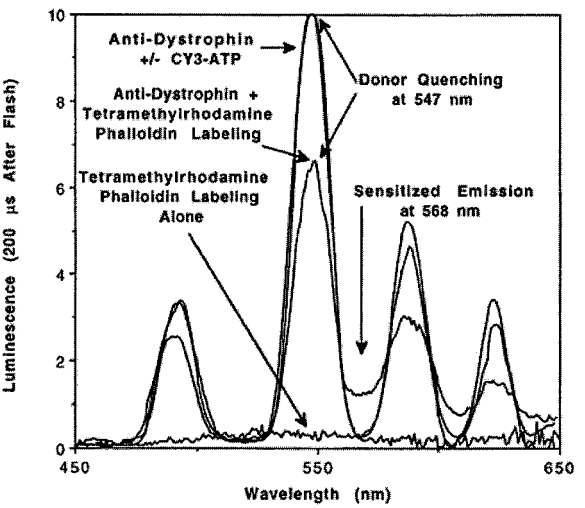

Figure 10 LRET signal indicating molecular proximity between dystrophin and actin in a muscle cell. [Figure from (46)].

distribution of donor-acceptor complexes: Donor-emission measurements are weighted toward those transferring less energy, and sensitized-emission measurements are weighted toward those transferring more energy. For example, if some donors have no acceptors nearby, this will lengthen the average donor lifetime, whereas it does not affect the sensitized-emission lifetime because this latter signal arises only from those complexes that can transfer energy.)

Root also looked at the spatial distribution of the anti-dystrophin antibodies by performing LRET in a microscope. Examining 90-μm diameter regions of the tissue sections, dual-labeled samples yielded a sensitized-emission lifetime of $0.7+/-0.1$ msec, but donor-emission lifetimes were more variable, ranging from 0.7 msec to 1.4 msec. Root suggested that the association for dystrophin for actin may have micro-heterogeneity within the cell.

Finally, Root compared the detection of molecular colocalization using LRET with the conventional technique of immunofluorescence colocalization. In immunofluorescence colocalization, the association of two objects are inferred by staining them with different dyes and looking for spatial overlap of the fluorescence from the two dyes in the microscope. This technique, although widely used, is limited in spatial resolution by conventional diffraction (submicron resolution) and therefore cannot differentiate between a true molecular association (nm scale) and nearby binding (submicron). Root looked for the association of dystrophin with nucleotide-binding proteins. Specifically, he stained muscle sections with the terbium-labeled anti-dystrophin antibody and with ATP bound to the dye Cy3, which is spectrally similar to tetramethylrhodamine. Both were found in the cell periphery by immunofluorescence microscopy, but no energy transfer was found, indicating that they were in the same vicinity but may not be molecularly interacting. Hence, the combination of using lanthanides as donors, which can produce significant energy transfer even with antibodies, and the extra spatial resolution of resonance energy transfer yields a more accurate picture of molecular interactions than conventional immunofluorescence microscopy.

APPLICATION 4: DETECTION OF BINDING IN HIGH-THROUGHPUT SCREENING

Biochemistry, at its fundamental level, is the interaction of macromolecular complexes. The detection of such events, and the ability to alter them through drugs, is essential for basic and applied science. With combinatorial chemical methods, it is now possible to produce millions of proto-drugs, and the ability to screen these rapidly, cheaply, and sensitively is crucial in drug development efforts. LRET has become increasingly popular for this purpose. LRET has several advantages. First, LRET is nonisotopic and hence avoids the health, environmental, and cost problems associated with radioactive assays, which historically have been standard. Second, LRET is homogenous, i.e., requires no separation or wash steps. Third, because LRET can measure fairly long distances, generic labeling reagents, which are often relatively large, can be used. This has the enormous advantage of being

able to use one or a few sets of labeling reagents (e.g., antibodies, streptavidin, Protein A) for many different assays. Fourth, the ability to detect relatively small amounts of energy transfer—generally through sensitized emission, which is sensitive to only donor-acceptor pairs—enables the analysis of samples that may have only a small percentage of fully labeled donor-acceptor pairs. This is particularly relevant when using complex mixtures such as cell extracts. Finally, LRET can be detected at (sub-) nanomolar concentrations, which minimizes reagent use and is often required if measuring the binding of nanomolar-affinity complexes.

Figure 11*a* highlights an assay to measure protein-protein interaction using generic reagents (34, 42). Jun and Fos oncogenes produce proteins that form a heterodimer. The dimer can bind to DNA and regulate transcription. Drugs that inhibit this dimerization are of potential therapeutic value. In one screening assay, a 40–amino acid section of Jun and of Fos, both containing the leucine zipper–binding domains responsible for dimerization, was synthesized and labeled with a biotin-avidin-chelate and the large fluorescent phycobiliprotein allophycocanin. Dimerization led to sensitized emission of the APC. Addition of an inhibitor disrupted dimerization and hence decreased APC-sensitized emission. Therefore screening for drugs that inhibit Jun-Fos dimerization can be readily achieved using LRET.

A second example using LRET and generic labels involves monitoring ligand-receptor interactions, which are often the first or early steps in a long biochemical cascade. In Figure 11*b*, an interleukin 4 (IL-4) ligand is biotinylated and then labeled with an APC-streptavidin (44). The IL-4 receptor (IL-4R) is expressed as a fusion protein with a Fc fragment. A europium-labeled protein-A is then used to label the Fc fragment of the IL-4R. The nanomolar-binding affinity for ligand and receptor is readily measured by changes in APC-sensitized emission.

FINAL REMARKS

New biophysical techniques invariably open up new applications. The development of new probes is leading to a dramatic expansion of the use of fluorescence in general and FRET-based techniques in particular. The most pressing issue is the ability to site-specifically label probes. Temporal and spectral discrimination when using lanthanides in energy transfer measurements help decrease the sensitivity to nonspecific labeling. However, particularly for cellular work, more selective means of attachments for both donors and acceptors are needed. Two different methods, one for donor, and one for acceptor, would be ideal. Genetically encoded dyes such as green fluorescent proteins is one method of selective attachment (56); dyes such as “FLASH,” which bind to a highly unusual six–amino acid motif via an arsenic moiety, is another (19); dyes modified to contain Ni, which can then coordinate to a hexahistidine group engineered into a protein, is yet another (31). Using the power of these new labeling methods with the

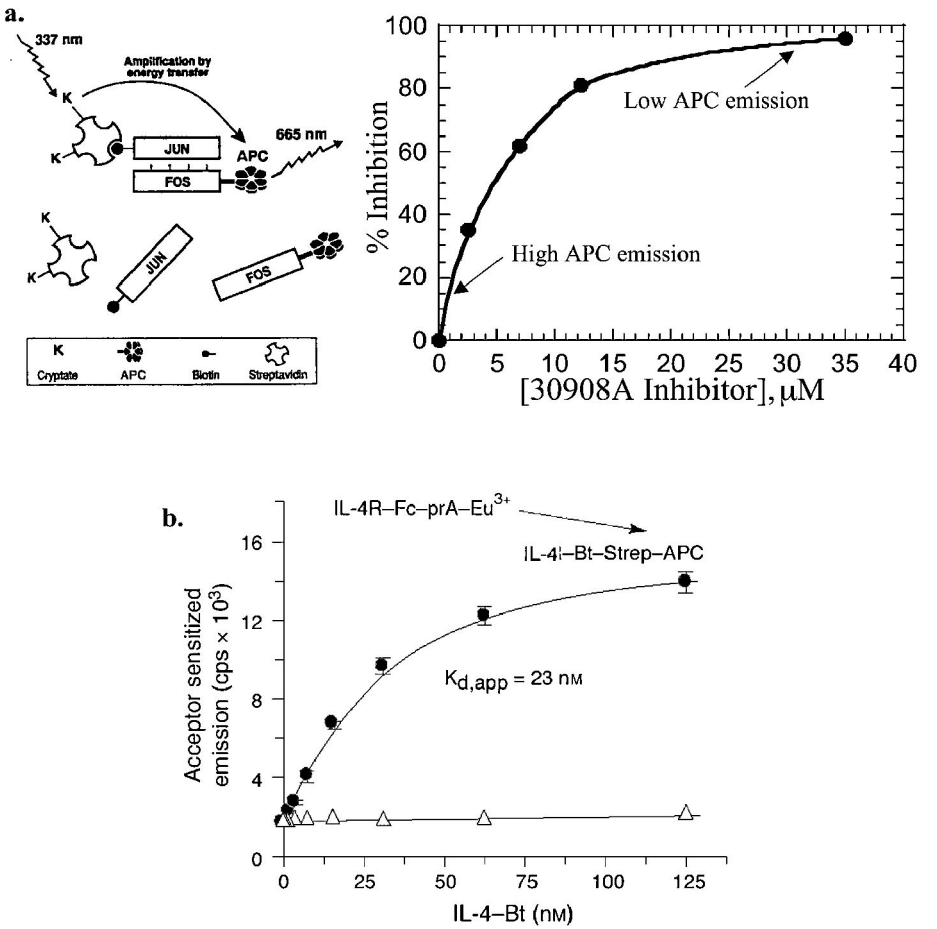

Figure 11 Measuring binding events for high-throughput screening assays using generic labeling reagents. (*a*) Jun-Fos dimerization and inhibition by drug. [Figure adapted from (34, 42)]. (*b*) Ligand-receptor binding in the IL-4 system with an apparent binding constant of 23 nM. [Figure from (44)].

power of lanthanides will likely shed new light on biophysical systems in the near future.

ACKNOWLEDGMENTS

I would like to thank Jeff Reifenberger for generating Table 1. This work was supported by NIH AR44420, NSF 9984841, and through the Material Research Laboratory, University of Illinois, DOE grant DEFG 02-91ER45439.

LITERATURE CITED

1. Blaustein RO, Cole PA, Williams C, Miller C. 2000. Tethered blockers as molecular 'tape measures' for a voltage-gated K+ channel. *Nat. Struct. Biol.* 7:309–11
2. Blomberg K, Hurskainen P, Hemmila I. 1999. Terbium and rhodamine as labels in a homogeneous time-resolved fluorometric energy transfer assay of the B subunit of human chorionic gonadotropin in serum. *Clin. Chem.* 45:855–61
3. Bunzli J-CG. 1989. Luminescent probes. In *Lanthanide Probes in Life, Chemical and Earth Sciences, Theory and Practice*, ed. J-CG Bunzli, GR Choppin, pp. 219–93. New York: Elsevier
4. Callaci S, Heyduk E, Heyduk T. 1999. Core RNA polymerase from *E. coli* induces a major change in the domain arrangement of the sigma 70 subunit. *Mol. Cell* 3:229–38
5. Cantor CR, Schimmel PR. 1980. *Biophysical Chemistry*. San Francisco: Freeman

5a. Cha A, Bezanilla. 1997. Characterizing voltage-dependent conformational changes in the Shaker K+ channel with fluorescence. *Neuron* 19(5):1127–40

6. Cha A, Snyder GE, Selvin PR, Bezanilla F. 1999. Atomic scale movement of the voltage sensing region in a potassium channel measured via spectroscopy. *Nature* 402:809–13
7. Chakrabarty T, Xiao M, Cooke R, Selvin PR. 2000. Structure and dynamics of the myosin dimer measured by fluorescence and luminescence resonance energy transfer. *Biophys. J.* 78:233A
8. Chen J, Selvin PR. 1999. Thiol-reactive luminescent lanthanide chelates. *Bioconjugate Chem.* 10:311–15
9. Chen J, Selvin PR. 2000. Lifetime and color-tailored fluorophores in the micro- to milli-second time regime. *J. Am. Chem. Soc.* 122:657–60
10. Clegg RM. 1995. Fluorescence resonance energy transfer. *Curr. Opin. Biotechnol.* 6:103–10
11. Clegg RM, Murchie AI, Zechel A, Lilley DM. 1993. Observing the helical geometry of double-stranded DNA in solution by fluorescence resonance energy transfer. *Proc. Natl. Acad. Sci. USA* 90:2994–98
12. Coker G III, Chen SY, van der Meer BW. 1994. *Resonance Energy Transfer*. New York: VCH
13. Cooper ME, Sammes PG. 2000. Synthesis and properties of a new luminescent europium(III) terpyridyl chelate. *J. Chem. Soc. Perkin Trans.* 28:1675–700
14. Dale RE, Eisinger J, Blumberg WE. 1979. The orientational freedom of molecular probes. *Biophys. J.* 26:161–94
15. Drexhage KH. 1970. Monomolecular layers and light. *Sci. Am.* 222:108–19
16. Fairclough RH, Cantor CR. 1978. The use of singlet-singlet energy transfer to study macromolecular assemblies. *Methods Enzymol.* 48:347–79
17. Farrar SJ, Whiting PJ, Bonnert TP, McKernan RM. 1999. Stoichiometry of a ligand-gated ion channel determined by fluorescence energy transfer. *J. Biol. Chem.* 274:10100–4
18. Glauner KS, Mannuzzu LM, Gandhi CS, Isacoff EY. 1999. Spectroscopic mapping of voltage sensor movement in the Shaker potassium channel. *Nature* 402:813–17
19. Griffin BA, Adams SR, Tsien RY. 1998. Specific covalent labeling of recombinant protein molecules inside live cells. *Science* 281:269–72
20. Helmann JD, deHaseth PL. 1999. Protein-nucleic acid interactions during open complex formation investigated by systematic alteration of the protein and DNA binding partners. *Biochemistry* 38:5959–67
21. Hemmilä I, Dakubu S, Mukkala V-M, Siitari H, Lövgren T. 1984. Europium as a

label in time-resolved immunofluorometric assays. *Anal. Biochem.* 137:335–43
22. Heyduk E, Heyduk T. 1997. Thiol-reactive luminescent Europium chelates: luminescence probes for resonance energy transfer distance measurements in biomolecules. *Anal. Biochem.* 248:216–27
23. Heyduk E, Heyduk T. 1999. Architecture of a complex between the sigma 70 subunit of *Escherichia coli* RNA polymerase and the nontemplate strand oligonucleotide. Luminescence resonance energy transfer study. *J. Biol. Chem.* 274:3315–22
24. Heyduk T, Heyduk E. 2001. Luminescence energy transfer with lanthanide chelates: interpretation of sensitized acceptor decay amplitudes. *Anal. Biochem.* 289:60–67
25. Heyduk E, Heyduk T, Claus P, Wisniewski JR. 1997. Conformational changes of DNA induced by binding of chironomus high mobility group protein 1a (cHMG1a). *J. Biol. Chem.* 272:19763–70
26. Horenstein J, Wagner DA, Czajkowski C, Akabas MH. 2001. Protein mobility and GABA-induced conformational changes in GABA(A) receptor pore-lining M2 segment. *Nat. Neurosci.* 4:477–85
27. Horn R. 2000. A new twist in the saga of charge movement in voltage-dependent ion channels. *Neuron* 25:511–14
28. Johnson JP Jr, Zagotta WN. 2001. Rotational movement during cyclic nucleotide-gated channel opening. *Nature* 412:917–21
29. Jones SG, Lee DY, Wright JF, Jones CN, Teear ML, et al. 2001. Improvements in the sensitivity of time resolved fluorescence energy transfer assays. *J. Fluoresc.* 11:13–21
30. Jovin TM, Arndt-Jovin DJ. 1989. FRET microscopy: digital imaging of fluorescence resonance energy transfer. Applications in cell biology. In *Microspectrofluorimetry of Single Living Cells*, ed. E Kohen, JS Ploem, JG Hirschberg, pp. 99–117. Orlando: Academic
31. Kapanidis AN, Ebright YW, Ebright RH. 2002. Site-specific incorporation of fluorescent probes into protein: hexahistidine-tag-mediated fluorescent labeling using (Ni++: nitrilotriacetic acid)n-fluorochrome conjugates. *J. Am. Chem. Soc.* 123 (48):12123–25
32. Kapanidis AN, Ebright YW, Ludescher RD, Chan S, Ebright RH. 2001. Mean DNA bend angle and distribution of DNA bend angles in the CAP-DNA complex in solution. *J. Mol. Biol.* 312:1–16
33. Karstens T, Kobs K. 1980. Rhodamine B and rhodamine 101 as reference substances for fluorescence quantum yield measurements. *J. Phys. Chem.* 84:1871–72
34. Kolb AJ, Burke JW, Mathis G. 1997. A homogeneous, time-resolved fluorescence method for drug discovery. In *High Throughput Screening: The Discovery of Bioactive Substances*, ed. JP Devlin, pp. 345–60. New York: Marcel Dekker
35. Lakowicz JR. 1999. *Principles of Fluorescence*. New York: Kluwer
36. Li M, Selvin PR. 1997. Amine-reactive forms of a luminescent DTPA chelate of terbium and europium: attachment to DNA and energy transfer measurements. *Bioconjugate Chem.* 8:127–32
37. Loo TW, Clarke DM. 2001. Cross-linking of human multidrug resistance p-glycoprotein by the substrate, tris-(2-maleimidoethyl)amine, is altered by atp hydrolysis. evidence for rotation of a transmembrane helix. *J. Biol. Chem.* 276:31800–5
38. Malhotra A, Severinova E, Darst SA. 1996. Crystal structure of a sigma 70 subunit fragment from *E. coli* RNA polymerase. *Cell* 87:127–36
39. Mannuzzu LM, Moronne MM, Isacoff EY. 1996. Direct physical measure of conformational rearrangement underlying potassium channel gating. *Science* 271:213–16
40. Marriott G, Heidecker M, Diamandis EP, Yan-Marriott Y. 1994. Time-resolved delayed luminescence image microscopy using an europium ion chelate complex. *Biophys. J.* 67:957–65
41. Mathis G. 1993. Rare earth cryptates and homogeneous fluoroimmunoassays with human sera. *Clin. Chem.* 39:1953–59

42. Mathis G. 1995. Probing molecular interactions with homogeneous techniques based on rare earth cryptates and fluorescence energy transfer. *Clin. Chem.* 41:1391–97
43. Mathis G, Socquet F, Viguier M, Darbouret B. 1997. Homogeneous immunoassays using rare earth cryptates and time resolved fluorescence: principles and specific advantages for tumor markers. *Anticancer Res.* 17:3011–14
44. Pope AJ, Haupts UM, Moore KJ. 1999. Homogeneous fluorescence readouts for miniaturized high-throughput screening: theory and practice. *Drug Discov. Today* 4: 350–62
45. Deleted in proof
46. Root DD. 1997. *In situ* molecular association of dystrophin with actin revealed by sensitized emission immuno-resonance energy transfer. *Proc. Natl. Acad. Sci. USA* 94:5685–90
47. Saha AK, Kross K, Kloszewski ED, Upson DA, Toner JL, et al. 1993. Time-resolved fluorescence of a new europium chelate complex: demonstration of highly sensitive detection of protein and DNA samples. *J. Am. Chem. Soc.* 115:11032–33
48. Sammes PG, Yahioglu G. 1996. Modern bioassays using metal chelates as luminescent probes. *Nat. Prod. Rep.* 13:1–28
49. Selvin PR. 1995. Fluorescence resonance energy transfer. *Methods Enzymol.* 246: 300–34
50. Selvin PR. 1996. Lanthanide-based resonance energy transfer. *IEEE J. Quantum Electron.* 2:1077–87
51. Selvin PR. 2000. The renaissance in fluorescence resonance energy transfer. *Nat. Struct. Biol.* 7:730–34
52. Selvin PR, Hearst JE. 1994. Luminescence energy transfer using a terbium chelate: improvements on fluorescence energy transfer. *Proc. Natl. Acad. Sci. USA* 91:10024–28
53. Seveus L, Vaisala M, Hemmila I, Kojola H, Roomans GM, Soini E. 1994. Use of fluorescent europium chelates as labels in microscopy allows glutaraldehyde fixation and permanent mounting and leads to reduced autofluorescence and good long-term stability. *Microsc. Res. Tech.* 28:149–54
54. Siitari H, Hemmila I, Soini E, Lövgren T, Koistinen V. 1983. Detection of hepatitis B surface antigen using time-resolved fluoroimmunoassay. *Nature* 301:258–60
55. Stenroos K, Hurskainen P, Eriksson S, Hemmila I, Blomberg K, Lindqvist C. 1998. Homogeneous time-resolved IL-2-IL-2R alpha assay using fluorescence resonance energy transfer. *Cytokine* 10:495–99
56. Stryer L, Haugland RP. 1967. Energy transfer: a spectroscopic ruler. *Proc. Natl. Acad. Sci. USA* 58:719–26
57. Stryer L, Thomas DD, Meares CF. 1982. Diffusion-enhanced fluorescence energy transfer. *Annu. Rev. Biophys. Bioeng.* 11: 203–22
58. Takalo H, Mukkala V-M, Mikola H, Liitti P, Hemmila I. 1994. Synthesis of europium(III) chelates suitable for labeling of bioactive molecules. *Bioconjugate Chem.* 5:278–82
59. Tsien RY. 1998. The green fluorescent protein. *Annu. Rev. Biochem.* 67:509–44
60. Vamosi G, Gohlke C, Clegg R. 1996. Fluorescence characteristics of 5-carboxytetramethylrhodamine linked covalently to the 5′ end of oligonucleotides: multiple conformers of single-stranded and double-stranded dye-DNA complexes. *Biophys. J.* 71:972–94
61. Weber G, Teale FWJ. 1957. Determination of the absolute quantum yield of fluorescent solutions. *Trans. Faraday Soc.* 53:646–55
62. Xiao M, Li H, Snyder GE, Cooke RG, Yount R, Selvin PR. 1998. Conformational changes between the active-site and regulatory light chain of myosin as determined by luminescence resonance energy transfer: the effect of nucleotides and actin. *Proc. Natl. Acad. Sci. USA* 95:15309–14
63. Xiao M, Selvin PR. 1999. An improved instrument for measuring time-resolved lanthanide emission and resonance energy transfer. *Rev. Sci. Inst.* 70:3877–81

64. Xiao M, Selvin PR. 2001. Quantum yields of luminescent lanthanide chelates and far-red dyes measured by resonance energy transfer. *J. Am. Chem. Soc.* 123:7067–73
65. Xu YY, Pettersson K, Blomberg K, Hemmila I, Mikola H, Lövgren T. 1992. Simultaneous quadruple-label fluorometric immunoassay of thyroid-stimulating hormone, 17 alpha-hydroxyprogesterone, immunoreactive trypsin, and creatine kinase MM isoenzyme in dried blood spots. *Clin. Chem.* 38:2038–43

Annual Review of Biophysics and Biomolecular Structure
Volume 31, 2002

CONTENTS